

Properties of gluino-gluino-gluon states

Seiji Ono

Physics Department, University of Tokyo, Tokyo 113, Japan

(Received 16 August 1984)

The spectra and decay properties of gluino-gluino-gluon ($\tilde{g}\tilde{g}g$) states are studied. It is shown that the lowest $\tilde{g}\tilde{g}g$ state is heavier than the lowest color-singlet gluino-gluino state $(\tilde{g}\tilde{g})_1$ by several GeV and the decay properties of the $\tilde{g}\tilde{g}g$ states are much different from those of $(\tilde{g}\tilde{g})_1$ states.

The gluino (\tilde{g}) is supposed to be one of the easiest supersymmetric particles to be found. Since the gluino is a color-octet state it cannot be observed directly. Some observable states which include the gluino(s) are (see, e.g., Refs. 1-6)

$$\tilde{g}g, \tilde{g}q\bar{q}, (\tilde{g}\tilde{g})_1, \tilde{g}\tilde{g}g. \quad (1)$$

The $(\tilde{g}\tilde{g})_1$ state can be produced either in heavy-quarkonium radiative decay or in hadronic processes through two gluons or directly from a quark line by exchanging a scalar quark. The produced $\tilde{g}\tilde{g}$ can be not only in a color-singlet state but also in a color-octet state.⁴ In the latter case the produced color-octet $\tilde{g}\tilde{g}$ will quickly pick up a soft quark pair or a soft gluon to become an observable color-singlet state. It is shown⁴ that such state can be copiously produced in $p\bar{p}$ scattering and can be identified.

In this paper we study the properties of the $\tilde{g}\tilde{g}g$ state (this is analogous to hybrid meson $Q\bar{Q}g$ and hybrid baryon $QQQg$). One might think that the properties of this state do not differ much from those for the $(\tilde{g}\tilde{g})_1$ state which has been already studied in detail.^{3,7-9} However, the interaction between two gluinos in a color-singlet state is twice as strong as that in a color-octet state because of the color factor:

$$F_{\tilde{g}\tilde{g}} \cdot F_{\tilde{g}\tilde{g}} = \begin{cases} -3 & \text{for singlet } \tilde{g}\tilde{g}, \\ -\frac{3}{2} & \text{for octet } \tilde{g}\tilde{g}. \end{cases} \quad (2)$$

More precisely the effective interaction between two gluinos should be determined in a specific model. We use here the bag model of Hasenfratz, Hogan, Kuti, and Richard.¹⁰ The detail of this model is explained in Ref. 11.

The gluino and the gluon carry Abelian charges of type I denoted by e and other Abelian charges of type Y denoted by q . In the $\tilde{g}\tilde{g}g$ system, $\tilde{g}\tilde{g}$ must be in a color octet and the whole system $\tilde{g}\tilde{g}g$ must be in a color singlet; thus, one finds

$$\begin{aligned} e &= \frac{3}{2}g, \quad q = \frac{\sqrt{3}}{2}g && \text{for the first gluino,} \\ e &= -\frac{3}{2}g, \quad q = \frac{\sqrt{3}}{2}g && \text{for the second gluino,} \\ e &= 0, \quad q = -\sqrt{3}g && \text{for the gluon.} \end{aligned} \quad (3)$$

The effective potential between two gluinos is derived in the Born-Oppenheimer approximation. In Refs. 10 and 11 the model was applied for the heavy hybrid system $Q\bar{Q}g$. In order to study the $\tilde{g}\tilde{g}g$ state we should only replace the color factor, i.e., Eq. (19) in Ref. 11 by Eq. (3) in this paper. The effective potential between two gluinos is computed by assuming that two gluinos and the transverse gluon are in a spherical bag with radius R . The constituent gluon occupies a definite quantum number in the spherical bag, i.e., stationary TE or TM mode. The total energy of the $\tilde{g}\tilde{g}g$ state includes the instantaneous Coulomb interaction energy ($\tilde{g}\tilde{g}$ and $\tilde{g}\tilde{g}$) of the color charge inside the bag. The potential is given by

$$\begin{aligned} V(r) &= \frac{4}{3}\pi R^3 \Lambda_B^4 + \frac{\alpha_{nj}^\lambda}{R} - \frac{3}{2} \frac{\alpha_s}{r} \\ &+ \frac{3\alpha_s}{2R} \left\{ \frac{2r^2}{4R^2 - r^2} - 2 \ln \left[1 - \frac{r^2}{4R^2} \right] + \frac{r^2}{4R^2 + r^2} \right. \\ &\quad \left. + \ln \left[1 + \left[\frac{r}{2R} \right]^2 \right] - 3 + \frac{r^2}{4R^2} + \frac{6}{5} \right\}, \end{aligned} \quad (4)$$

where the last term $9\alpha_s/5R \equiv E_{gg}$ is the gluon self-energy term. The bag radius R is determined by the minimization condition $\partial V/\partial R = 0$ for given r . The r is the distance between two gluinos, the first term is the volume energy and the second term is the energy of gluon in a specific mode. We compute only the lowest gluon mode (TE) which corresponds to $\alpha^{\text{TE}} = 2.744$.

The radial wave function $\psi(r)$ between two gluinos $(\tilde{g}\tilde{g})_8$ is calculated by the Schrödinger equation

$$-\frac{1}{M_{\tilde{g}}} \frac{d^2}{dr^2} \psi(r) + \frac{1}{M_{\tilde{g}}} \frac{\langle (\mathbf{L}-\mathbf{j})^2 \rangle}{r^2} \psi(r) + V(r)\psi(r) = E\psi(r), \quad (5)$$

$$\langle (\mathbf{L}-\mathbf{j})^2 \rangle = L(L+1) + j(j+1) - 2\Lambda^2,$$

where \mathbf{L} is the total orbital angular momentum and \mathbf{j} is the angular momentum of gluon ($j=1$ for the lowest TE). Λ is the eigenvalue for the projection of the gluon's angular momentum along the two gluino axis.

We show two models to classify the $\tilde{g}\tilde{g}g$ states. In the first model we use the similarity of this state to diatomic molecule as in Ref. 10. We neglect the spin-dependent force, thus the energy level depends only on the value of $\langle (\mathbf{L}-\mathbf{j})^2 \rangle$ and the number of radial nodes of the wave

function. The quantum numbers of $\tilde{g}\tilde{g}g$ states in each level in this model are exactly the same as those for hybrid meson $Q\bar{Q}g$ which are already described in Refs. 10 and 11 and we do not repeat here. Following Ref. 11 we name the energy levels in the following way according to the expectation value of $\langle(L-j)^2\rangle$:

$$\langle(L-j)^2\rangle = \begin{cases} 2, & 1A, 2A, 3A, \dots, \\ 4, & 1B, 2B, 3B, \dots, \\ 6, & 1C, 2C, 3C, \dots \end{cases} \quad (6)$$

We do not know for sure if the above model is appropriate for $\tilde{g}\tilde{g}g$ states. Is the $\tilde{g}\tilde{g}g$ state really so similar to the diatomic molecule? In case of the diatomic molecule the motion of the electron is very much restricted to the axis of two nucleons, thus it is better to introduce a coordinate system which is moving together with two nucleons. On the other hand, the bag radius for $\tilde{g}\tilde{g}g$ state ($R \sim 0.4$ fm) is much larger than the distance between two gluinos (~ 0.04 fm). This means that two gluinos are well concentrated near the center and the wave function of the gluon is not much disturbed by the finite size of two gluinos. Therefore, the $\tilde{g}\tilde{g}$ axis does not play an important role for the gluon wave function.

In the second model for the $\tilde{g}\tilde{g}g$ classification we assume that the gluon inside the bag is free. The total wave function is simply the product of the $(\tilde{g}\tilde{g})_8$ wave function and the free gluon wave function. The motion of the gluon decouples from that of the $(\tilde{g}\tilde{g})_8$ state. In this model the lowest state for $(\tilde{g}\tilde{g})_8$ is simply 1S state and the

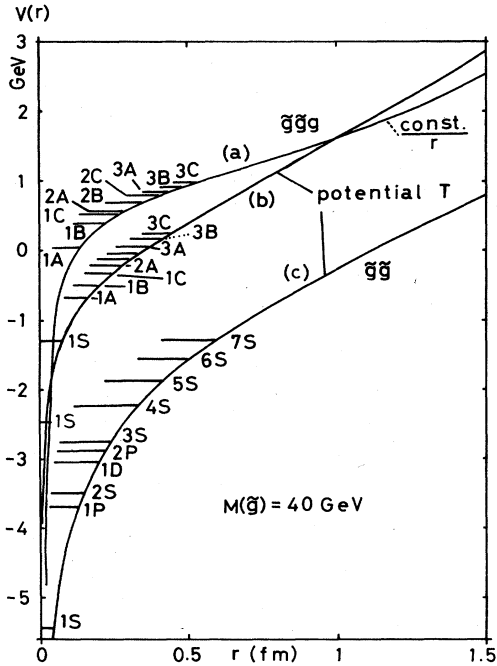


FIG. 1. The energy spectra and potentials for $\tilde{g}\tilde{g}g$ and $(\tilde{g}\tilde{g})_1$ states. (a) $(\tilde{g}\tilde{g})_8$ potential given by Eq. (4). (b) Same as (a) but $-3\alpha_s/2r$ is replaced by potential T [Eq. (8)]. (c) $(\tilde{g}\tilde{g})_1$ potential.

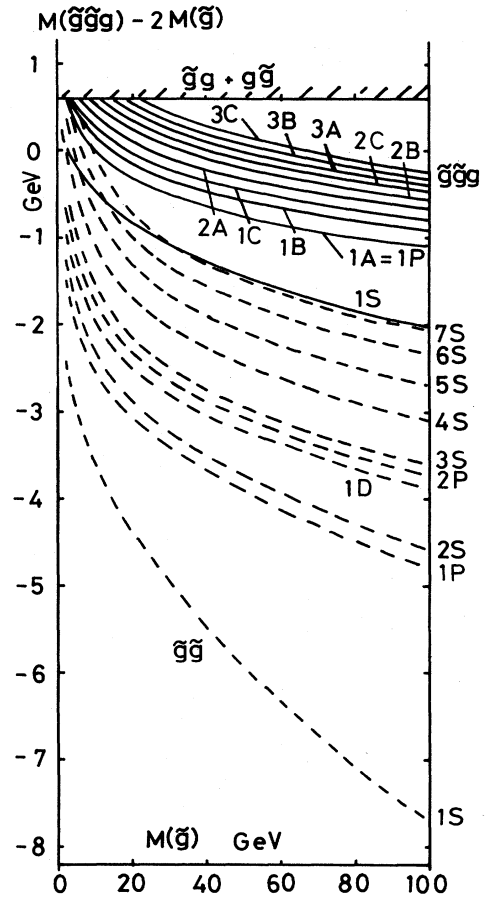


FIG. 2. The energy spectra for $\tilde{g}\tilde{g}g$ states (solid curves) and for $(\tilde{g}\tilde{g})_1$ states (dashed curves).

next one is the 1P state and so on. On the other hand, we find $\langle(L-j)^2\rangle \geq 2$ for the TE mode in the first model, i.e., the $(\tilde{g}\tilde{g})_8$ cannot be in an S state in this sense. Energy levels in two models are compared in the following:

$\langle(L-j)^2\rangle$	Model 1	Model 2
0	forbidden	allowed (1S)
2	allowed (1A)	allowed (1P)
4	allowed (1B)	forbidden
6	allowed (1C)	allowed (1D)

(7)

In model 2 the lowest energy level is the 1S state, which is lower than the 1A state by around 200 MeV, which is still

TABLE I. The quantum numbers of $(\tilde{g}\tilde{g})_8$ state inside $\tilde{g}\tilde{g}g$ state.

Color antisymmetric		Color symmetric	
3S_1	$J^P=1^-$	1S_0	$J^P=0^-$
1P_1	$J^P=1^+$	$^3P_{0,1,2}$	$J^P=0^+, 1^+, 2^+$
$^3D_{1,2,3}$	$J^P=1^-, 2^-, 3^-$	1D_2	$J^P=2^-$

TABLE II. Some of the decay processes of color-octet $(\tilde{g}\tilde{g})_8$ states and the decay-rate formulas. Color factors are $C_1 = \frac{3}{8}$, $C_2 = \frac{3}{4}$, and $C_3 = \frac{9}{8}$, where C_2 and C_3 contain a factor one-half which comes from the Majorana nature of the gluino. In order to obtain quarkonium and $(\tilde{g}\tilde{g})_1$ decay rates into gg one should replace C_3 by $\frac{2}{3}$ and $\frac{9}{2}$, respectively.

Process	Decay rate
$[^3S_1, (\tilde{g}\tilde{g})_8] \rightarrow [^3P_J, (\tilde{g}\tilde{g})_1] + g$	$\frac{4}{3} \frac{2J+1}{9} C_1 \alpha_s k^3$ $\times \left[\int r^2 dr R_{(\tilde{g}\tilde{g})_1} r R_{(\tilde{g}\tilde{g})_8} \right]^2$
$\rightarrow [^1S_0, (\tilde{g}\tilde{g})_1] + g$	$\frac{4}{3} C_1 \frac{\alpha_s k^3}{m_{\tilde{g}}^2}$ $\times \left[\int r^2 dr R_{(\tilde{g}\tilde{g})_1}(r) j_0 \left(\frac{kr}{2} \right) R_{(\tilde{g}\tilde{g})_8}(r) \right]^2$
$\rightarrow g \rightarrow Q\bar{Q}$	$C_2 \frac{\alpha_s^2}{3m_{\tilde{g}}^2} R(0) ^2$
$[^1S_0, (\tilde{g}\tilde{g})_8] \rightarrow gg$	$C_3 \frac{\alpha_s^2}{m_{\tilde{g}}^2} R(0) ^2$
$[^1P_1, (\tilde{g}\tilde{g})_8] \rightarrow [^1S_0, (\tilde{g}\tilde{g})_1] + g$	$\frac{4}{9} C_1 \alpha_s k^3$ $\times \left[\int r^2 dr R_{(\tilde{g}\tilde{g})_8} r R_{(\tilde{g}\tilde{g})_1} \right]^2$
$[^1P_1, (\tilde{g}\tilde{g})_8] \rightarrow [^1S_0, (\tilde{g}\tilde{g})_1] + g$	$\frac{12}{5} C_3 \frac{\alpha_s^2}{m_{\tilde{g}}^4} R'(0) ^2$
$\Gamma(^3P_0 \rightarrow gg) : \Gamma(^3P_2 \rightarrow gg) = 15:4$	

higher than the lowest $(\tilde{g}\tilde{g})_1$ state by several GeV.

Another theoretical ambiguity comes from the choice of the $(\tilde{g}\tilde{g})_8$ potential. In Eq. (4) the term $-3\alpha_s/2r$ dominates near the origin. In practice, this term is the most important one because the wave function for $(\tilde{g}\tilde{g})_8$ becomes very small for $\tilde{g}\tilde{g}$ state as $M(\tilde{g})$ becomes large. This situation is very similar to heavy-quarkonium case. As is well known it is not appropriate to use the simple Coulomb-type potential for the short-range region. Kühn and myself¹² proposed a potential (this is called potential T)

$$V(r) = -\frac{16\pi}{25} \frac{1}{rf(r)} \left[1 + \frac{2\gamma_E + \frac{53}{75}}{f(r)} - \frac{462 \ln f(r)}{625 f(r)} \right] + a\sqrt{r} + c,$$

$$f(r) \equiv \ln[1/(\Lambda_{\overline{MS}} r)^2 + b], \quad (8)$$

$$\Lambda_{\overline{MS}} = 140 \text{ MeV}, \quad a = 0.63 \text{ GeV}^{3/2},$$

$$b = 20, \quad c = -1.39 \text{ GeV}$$

TABLE III. Typical theoretical values of decay rates (in MeV). Other decay rates can be computed simply by replacing the color factor as shown in Table II.

$m_{\tilde{g}}$ (GeV)	5	10	20	40	60	80	100
$\Gamma(^3S_1(\tilde{g}\tilde{g})_8 \rightarrow Q\bar{Q})$	0.43	0.27	0.21	0.19	0.19	0.20	0.21
$\Gamma(^1S_0(\tilde{g}\tilde{g})_8 \rightarrow gg)$	7.76	4.88	3.73	3.39	3.46	3.61	3.75
$\Gamma(^3P_2(\tilde{g}\tilde{g})_8 \rightarrow gg)$	0.29	6.95×10^{-2}	2.09×10^{-2}	8.22×10^{-2}	5.43×10^{-3}	4.30×10^{-3}	3.70×10^{-3}
$\sum_{J=1}^3 \Gamma(^3S_1(\tilde{g}\tilde{g})_8 \rightarrow ^3P_J + g)$	227	158	92.3	46.5	29.3	20.7	15.8
$\Gamma(^3S_1(\tilde{g}\tilde{g})_8 \rightarrow ^1S_0 + g)$	25.1	10.2	4.01	1.68	1.06	0.79	0.64
$\Gamma(^1P_1(\tilde{g}\tilde{g})_8 \rightarrow ^1S_0 + g)$	239	130	60.8	30	20.6	16.9	14.3

(\overline{MS} denotes the modified minimal-subtraction scheme), which reproduces $c\bar{c}$ and $b\bar{b}$ spectra nicely and has short-range behavior predicted by a perturbative two-loop calculation.¹³

In Fig. 1 [curve (a)] we show the $(\tilde{g}\tilde{g})_8$ potential given by Eq. (4) after minimization with respect to R . In Fig. 1 [curve (b)] we plot a potential which is obtained by replacing $-3\alpha_s/2r$ part by potential T [Eq. (8)] after a suitable change of the color factor. For comparison we plot the $(\tilde{g}\tilde{g})_1$ potential [curve (c)]. As expected, the potential for $(\tilde{g}\tilde{g})_1$ is much more attractive than that for $(\tilde{g}\tilde{g})_8$ in $\tilde{g}\tilde{g}g$. We show also energy spectra of $\tilde{g}\tilde{g}g$ and $(\tilde{g}\tilde{g})_1$ for $M(\tilde{g})=40$ GeV.

We now consider the classification of $\tilde{g}\tilde{g}g$ state in the second model. In case of the $(\tilde{g}\tilde{g})_1$ state antisymmetry of the wave function requires $L+S$ to be even, i.e., $^1S_0, ^3P_J, ^1D_2$ are allowed and $^3S_1, ^1P_1, ^3D_J$ are forbidden. For the $(\tilde{g}\tilde{g})_8$ inside the $\tilde{g}\tilde{g}g$ state both $L+S=\text{even}$ and odd are allowed since the color factor can be antisymmetric as well as symmetric. Thus, the lowest states are $0^-, 1^-, 2^-$. In Table I we show quantum numbers and color symmetry for $(\tilde{g}\tilde{g})_8$ inside $\tilde{g}\tilde{g}g$.

One must add a soft gluon to these systems in order to obtain an observable $\tilde{g}\tilde{g}g$ state. This soft gluon couples to two gluons or a light-quark pair to induce the decay process $\tilde{g}\tilde{g}g \rightarrow (\tilde{g}\tilde{g})_1 + (\tilde{g}\tilde{g})_1$ or $\tilde{g}q\bar{q} + \tilde{g}q\bar{q}$ if these are kinematically allowed. There are some theoretical estimations for masses of $(\tilde{g}\tilde{g})_1$ and $\tilde{g}q\bar{q}$ states. We show only the lowest state:

$$\begin{aligned} M(\tilde{g}\tilde{g})_1 &\sim M(\tilde{g}) + 300 \text{ MeV} \\ &\quad \text{in Bethe-Salpeter (BS) model}^2, \\ M(\tilde{g}\tilde{g}_{TE})_1 &\sim M(\tilde{g}) + 480 \text{ MeV in bag model}^1, \\ M(\tilde{g}q\bar{q}) &\sim M(\tilde{g}) - 220 \text{ MeV in potential model}^{14}, \\ M(\tilde{g}q\bar{q}) &\sim M(\tilde{g}) + 600 \text{ MeV in BS model}^2. \end{aligned} \quad (9)$$

From these results one can conclude that the decay process $\tilde{g}\tilde{g}g \rightarrow (\tilde{g}\tilde{g})_1 + (\tilde{g}\tilde{g})_1$ is kinematically forbidden for low-lying $\tilde{g}\tilde{g}g$ states. As for $\tilde{g}\tilde{g}g \rightarrow \tilde{g}q\bar{q} + \tilde{g}q\bar{q}$ transition due to the theoretical ambiguity it is difficult to conclude if it is kinematically allowed.

The $(\tilde{g}\tilde{g})_8$ inside the $\tilde{g}\tilde{g}g$ state can couple to the gluon leaving the constituent soft gluon as a spectator. Since this gluino pair is a color-octet state it can annihilate into one or two gluons or it can make a transition into color-singlet $\tilde{g}\tilde{g}$ state emitting a color-octet gluon. The decay rate of A $(\tilde{g}\tilde{g})_8 \rightarrow (\tilde{g}\tilde{g})_1 + g$ is larger than the rates for (B) $(\tilde{g}\tilde{g})_8 \rightarrow g \rightarrow gg$, $(\tilde{g}\tilde{g})_8 \rightarrow gg$ (direct). For the color-

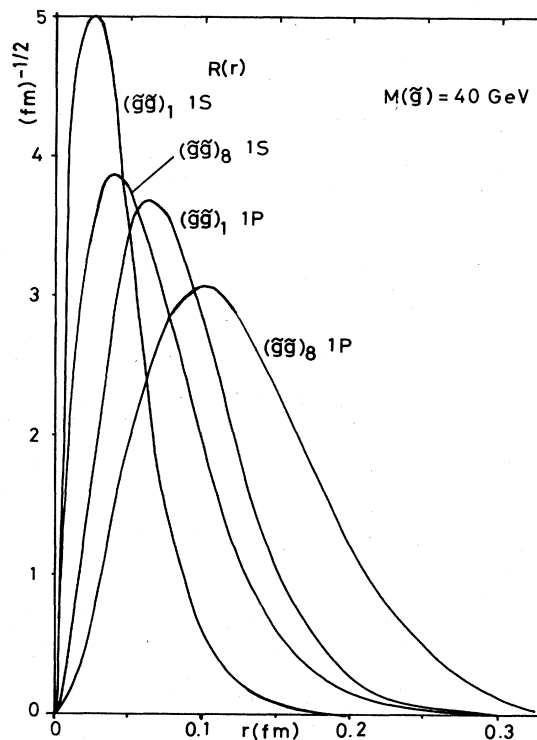


FIG. 3. Wave functions $R(r)$ for $\tilde{g}\tilde{g}$ inside $(\tilde{g}\tilde{g})_1$ and $\tilde{g}\tilde{g}g$. The normalization condition is $\int R(r)^2 dr = \int u(r)^2 r^2 dr = 1$.

antisymmetric $\tilde{g}\tilde{g}g$ states both types of decay are allowed and the (A) dominates while for the color-symmetric $\tilde{g}\tilde{g}g$ states only (A) is allowed and this becomes important.

Formulas and typical numerical numbers for these decay rates are shown in Tables II and III. From these values we find the following results:

- (i) $\tilde{g}\tilde{g}g$ states are much narrower than the $(\tilde{g}\tilde{g})_1$ states.
- (ii) The transition process into $(\tilde{g}\tilde{g})_1$ become the dominant decay mode for the color-antisymmetric $\tilde{g}\tilde{g}g$ states ($^3S_1, ^1P_1, \dots$). This is characterized by a monochromatic gluon jet.
- (iii) The color-symmetric $\tilde{g}\tilde{g}g$ states have much longer lifetime. For these states two-gluon decay becomes important before it is overtaken by a single-gluino decay process $\tilde{g} \rightarrow q\bar{q}\tilde{\gamma}, g\tilde{\gamma}$ which becomes important for large gluino mass.^{5,6}

The author would like to thank S. Yazaki, H. Kühn, and K. Higashijima for discussions.

¹D. V. Nanopoulos, S. Ono, and T. Yanagida, Phys. Lett. **137B**, 363 (1984).

²A. N. Mitra and S. Ono, Z. Phys. C **25**, 245 (1984).

³J. H. Kühn and S. Ono, Phys. Lett. **142B**, 436 (1984).

⁴H. E. Haber, in Proceedings of the DPF Workshop on $p\bar{p}$ Op-

tions for the Supercollider, 1984 (unpublished).

⁵H. E. Haber and G. L. Kane, Phys. Rep. (to be published).

⁶S. Ono, lecture presented at International Conference on Elementary Particle Physics, Hadron Structure '83, Smolenice, Czechoslovakia, 1983 (unpublished).

- ⁷T. Goldman and H. E. Haber, *Physica (Utrecht) D* (to be published).
- ⁸J. H. Kühn, *Phys. Lett.* **141B**, 433 (1984).
- ⁹W.-Y. Keung and A. Khare, *Phys. Rev. D* **29**, 2657 (1984).
- ¹⁰P. Hasenfratz, R. R. Horgan, J. Kuti, and J. M. Richard, *Phys. Lett.* **22B**, 299 (1980).
- ¹¹S. Ono, *Z. Phys. C* (to be published); talk at XIXth Rencontre de Moriond, New Particle Production at High Energies, La Plagne, Savoie, France, 1984 (unpublished).
- ¹²J. H. Kühn and S. Ono, *Z. Phys. C* **21**, 395 (1984).
- ¹³W. Buchmüller and S.-H. Tye, *Phys. Rev. D* **24**, 132 (1981).
- ¹⁴F. Schöberl, P. Falkensteiner, and S. Ono, *Phys. Rev. D* **30**, 603 (1984).